UNCLASSIFIED

AD 296 954

Reproduced
by the

ARMED SERVICES TECHNICAL INFORMATION AGENCY
ARLINGTON HALL STATION
ARLINGTON 12, VIRGINIA

UNCLASSIFIED

NOTICE: When government or other drawings, specifications or other data are used for any purpose other than in connection with a definitely related government procurement operation, the U. S. Government thereby incurs no responsibility, nor any obligation whatsoever; and the fact that the Government may have formulated, furnished, or in any way supplied the said drawings, specifications, or other data is not to be regarded by implication or otherwise as in any manner licensing the holder or any other person or corporation, or conveying any rights or permission to manufacture, use or sell any patented invention that may in any way be related thereto.

63-2-7

RADC-TDR-63-17

296954

CATALOGED BY ASTIA
AS AD No. 296954

296 954

A NONUNIFORMLY DISTRIBUTED PARAMETER MATCHING NETWORK FOR THE MICROWAVE FREQUENCIES

Daniel J. Kenneally

TECHNICAL DOCUMENTARY REPORT NO. RADC-TDR-63-17
January 1963

765700

Applied Research Laboratory
Rome Air Development Center
Research and Technology Division
Air Force Systems Command
Griffiss Air Force Base, New York

ASTIA
FEB 28 1963

Project No. 8505

Qualified requestors may obtain copies from the ASTIA Document Service Center, TISIA-2, Arlington Hall Station, Arlington 12, Virginia. Orders will be expedited if placed through the librarian or other person designated to request documents from ASTIA.

When U.S. Government drawings, specifications, or other data are used for any purpose other than a definitely related government procurement operation, the government thereby incurs no responsibility nor any obligation whatsoever; and the fact that the government may have formulated, furnished, or in any way supplied said drawings, specifications, or other data is not to be regarded by implication or otherwise, as in any manner licensing the holder or any other person or corporation, or conveying any rights or permission to manufacture, use, or sell any patented invention that may in any way be related thereto.

This document made available for study upon the understanding that the U.S. Government's proprietary interests in and relating thereto, shall not be impaired. In case of apparent conflict between the government's proprietary interests and those of others, notify the Staff Judge Advocate, Air Force Systems Command, Andrews Air Force Base, Washington 25, D.C.

Do not return this copy. Retain or destroy.

FOREWORD

The purpose of this report is to present the results of a theoretical and experimental analysis of a section of tapered coaxial waveguide, whose characteristic impedance is a cosinusoidal function of the axial coordinate. The feasibility of exploiting the proposed distribution in microwave impedance transformer is considered and mathematically confirmed. The theoretically predicted performance of such a transformer is compared with the test results of the experimental design with favorable results.

The theoretical phase of this effort was initially supported by Project 8505 and the engineering development phase was finally supported by Project 5578. The author is singularly indebted to Dr. Gorden Kent of Syracuse University for his encouraging counsel and helpful suggestions during the course of this investigation. Sincere appreciation for the timely and stimulating discussions on the various aspects of the theory goes to Mr. Haywood Webb, 8505 Project Engineer. Special thanks are due to co-workers Mr. Edward J. Calucci and Mr. Robert L. Dondero for time and talent freely given during the actual experimentation. Mr. John Altieri is also gratefully acknowledged for his participation in the design of various ancillary equipment.

This report was originally submitted by the author in partial fulfillment of the requirements for the degree of Master of Electrical Engineering at Syracuse University.

ABSTRACT

A nonuniform section of coaxial transmission line is investigated as an impedance matching network. Assuming that the purity of the dominant transverse electromagnetic (TEM) mode is maintained, the coaxial transformer section proposed is one in which the distributed series inductance and shunt capacitance are prescribed mathematical functions of the axial cylindrical coordinate, that is, the direction of propagation. These variations are expressed as a variable characteristic impedance in the explicit form of a half-period cosinusoidal distribution.

Starting with the appropriate differential equations for the nonuniform line voltages and currents, the basic Riccati-type differential equation governing the reflection coefficient in a nonuniform section is presented. In a conventional manner, an expression is then developed for the complex reflection coefficient at the input reference plane when the output port is terminated in a matched load. For given ranges in design parameters the magnitude of this integral expression is evaluated for this specific taper-cosinusoidal. The integration was performed on a Burrough's Datatron 205 computer using a Gaussian quadrature technique. From predicted performances, it appears that the cosinusoidal distribution offers "significant" improvement over conventional tapers, that is, linear, exponential, hyperbolic tangent, and Bessel. The apparent improvement is in terms of more effective matching over increased bandwidths.

The network itself is realized by machine tapering the inner conductor of a coaxial line in the mathematically prescribed manner within ±0.5 mil accuracy. The experimental unit is designed to corroborate the predicted performance for an arbitrarily chosen mismatch of 0.50 voltage (unmatched) reflection coefficient. A measurement procedure is presented and the results discussed in terms of experimental measurement accuracies, approximate theory, and over-all compatibility between theory and experiment.

PUBLICATION REVIEW

This report has been reviewed and is approved.

Approved: Milton Klaus
for DAVID F. BARBER
Chief, Applied Research Laboratory
Directorate of Engineering

Approved: Joseph J. Marecky
for WILLIAM F. BETHKE
Director of Engineering

FOR THE COMMANDER: Irving J. Gabelman
IRVING J. GABELMAN
Director of Advanced Studies

TABLE OF CONTENTS

Contents *Page*

I. INTRODUCTION 1
II. THE NONUNIFORM LINE EQUATIONS 2
III. THE COSINUSOIDAL TAPERED TRANSFORMER 5
IV. THEORETICAL RESULTS 18
V. EXPERIMENTAL ANALYSIS 20
VI. CONCLUSIONS 29
REFERENCES 30
BIBLIOGRAPHY 31
APPENDIX 32

LIST OF ILLUSTRATIONS

Figure *Page*

1. Taper Contour and Impedance Distribution 6
2-6. The Magnitude of the Normalized Reflection Coefficient versus the Ratio, Physical Length/Wavelength for ρ_0 = 0.1 to 0.5 8-12
7-11. Figures 2-6 Renormalized with the Consistent ρ_0 13-17
12. Comparative Transformer Performance for a 50 percent Mismatch 21
13a. Photograph of the Inner Conductor of the Cosinusoidal Transformer 23
13b. Engineering Drawing of Inner Conductor 24
14. Experimental Block Diagram for the Measurement of the Transformer Scattering Matrix 26
15. Comparison of Theoretical and Experimental Results for a 50 percent Mismatch 27

A NONUNIFORMLY DISTRIBUTED PARAMETER MATCHING NETWORK FOR THE MICROWAVE FREQUENCIES

I. INTRODUCTION

The advent of precision microwave radar during the late 1930's and early 1940's brought to the radio engineering community stringent requirements on transmitter and receiver efficiencies. In particular, there arose a demand for extremely well-matched microwave components, not only at the design frequencies, but over the large bandwidths dictated by the pulse ranging technique. One of the early methods of realizing such broadband impedance matches involved the use of sections of line with gradually changing cross sectional dimensions. This technique of tapered transitions remains quite popular even today. The tapered section of line is essentially a nonuniformly distributed parameter circuit whose series impedance per unit length and shunt admittance per unit length are both continuous functions of the axial coordinate. This variable, together with the appropriate time dependency, constitutes the independent variables that appear in the transmission line wave equations. For the nonuniform case, the wave equations are similar to the uniform case except that the coefficients of the partial derivatives are functions of the independent variable which specifies the direction of propagation.

The analysis of nonuniform transmission lines has been a subject of interest for a considerable period of time, not only to the microwave engineer but to others. For example, the wave equations for the dominant mode on a nonuniformly distributed coaxial line can be separated in the field variables, becoming similar in format to the one dimensional Schroedinger Wave Equations of Quantum Theory. Furthermore, the design of acoustic absorbers for sonar camouflage may use a nonuniform distribution of appropriate media. The analogous radar problem also may use a nonuniform lossy medium for aircraft camouflage. Consequently, in keeping with goals for an RADC project, which is aimed at continually improving the performance of microwave components, a study of impedance matching was undertaken. In particular, the use of sections with continuously varying dimensions to achieve the requisite reflectionless junction was heavily emphasized.

As a result of this study, there evolved one particular distribution which offers considerable improvement in over-all transformer performance compared to "conventional" tapers. It is one in which the distributed immitances are such that the characteristic impedance is a cosinusoidal function of the direction of propagation of a microwave coaxial line. This report treats the theoretical and experimental analysis of such a nonuniform transmission line when used as an impedance transformer to match two uniform lossless transmission lines with real and different characteristic impedances.

From the theoretical results and the corroborating experimental data, it is evident that the cosinusoidal transformer represents a significant improvement in the state of the art. In particular, for those applications in aerospace electronics demanding the maximum in transformer bandwidth in a minimum physical length, the cosinusoidal design

would appear very attractive. Consider, for example, a telemetry problem in which an unmanned orbiting data acquisition satellite is interrogated by an earth station or a manned space vehicle. Upon command, this satellite is to begin the transmission of the various data stored in its memory. The transmitting antenna for this purpose may require an impedance matching network for efficient coupling to the transmission line in the data acquisition satellite. The information capacity will determine the required bandwidth and, in all likelihood, will require as large a bandwidth as possible. Thus, because of the large information capacities involved and the obvious volume limitations, a transformer with maximum bandwidth and minimum length is indicated. The cosinusoidal design offers one possible solution to this problem.

II. THE NONUNIFORM LINE EQUATIONS

Consider an infinite transmission line with a distributed series impedance and a distributed shunt admittance, both of which are arbitrary functions of the longitudinal dimension. Assume that the propagating electromagnetic mode is the dominant configuration and, as such, the electric and magnetic fields are pure transverse (TEM). Proceeding in the classical manner[1,2,3] it is possible to show that the steady state voltage and current on such a transmission line satisfy the differential equations:

$$\frac{dV}{dx} = -ZI, \tag{1}$$

$$\frac{dI}{dx} = -YV, \tag{2}$$

where V is the voltage across the line,

I is the current in the line,

Z is the series impedance per unit length,

Y is the shunt admittance per unit length,

and all these parameters are functions of the propagation dimension x with the sinusoidal time variations in voltage and current being omitted for simplicity (total derivatives rather than partial). Elimination of one of the two dependent variables from equations (1) and (2) follows simply by differentiation of either equation and successive substitution. Thus, for example, from equation (1):

$$\frac{d^2V}{dx^2} = -\left(Z\frac{dI}{dx} + I\frac{dZ}{dx}\right),$$

and, upon substitution of equations (1) and (2),

$$\frac{d^2V}{dx^2} = YZV + \left(\frac{1}{Z}\frac{dV}{dx}\frac{dZ}{dx}\right),$$

or

$$\frac{d^2V}{dx^2} - YZV - \frac{d}{dx}(\ln Z)\frac{dV}{dx} = 0. \tag{3}$$

Similarly, the elimination of the voltage variable results in:

$$\frac{d^2I}{dx^2} - YZI - \frac{d}{dx}(\ln Y)\frac{dI}{dx} = 0. \tag{4}$$

Equations (3) and (4) represent the essence of the general problem in nonuniform transmission line theory. In the general analysis problem, the series impedance and shunt admittance are specified functions, $Z(x)$ and $Y(x)$, respectively, each being everywhere differentiable and containing no singularities at the origin. The problem, then, is to effect a solution of equations (3) and (4) subject to the above immittance restrictions and whatever boundary or end conditions may be present. For example, in the classical theory of transmission lines, the immittance distributions are simply constants and independent of x. In that case, three kinds of constants are of usual interest: pure real for absorbing lines in which $Z = R$ and $Y = G$, complex for lossy propagating lines in which $Z = R + jX$ and $Y = G + jB$, and pure imaginery for lossless propagating lines in which $Z = jX$ and $Y = jB$. For these three specialized cases, equations (1) and (2) become the well-known differential equations of classical line theory sometimes referred to as the Telegraphers' Equations.

Returning to the general case when $Z(x)$ and $Y(x)$ are arbitrary functions, the differential equations of the line are second order, linear equations with coefficients that are functions of the independent variable x. Except for some special cases yielding infinite series solutions in well-known, tabulated functions, these differential equations do not admit explicit solutions in closed form. Aside from the analytic arguments essential to the existence (of solutions) theorems, one must resort to numerical or graphical methods to extract practical engineering results.

Some of the special cases are those in which the impedance and admittance distributions are such that equations (3) and (4) become recognizable differential equations of mathematical physics. For example, in the so-called "exponential line,"[4,5]

$$Z \propto e^{-ax}, \quad Y \propto e^{+ax},$$

resulting in second order equations with constant coefficients which permit exponential solutions in voltage and current. In the so-called "Bessel line,"[6] both Z and Y are power functions of the independent variables resulting in various forms of Bessel's differential equation which permit a series solution for voltage and current in terms of Bessel functions.

Some of the other distributions that fall into the above category and, as such, have been studied in some detail are linear[7] and parabolic.[8] In all these cases, there is confusion concerning the authors' nomenclature for the particular line studied. Some,[7,8] for example, identify the line by the explicit functional form that the appropriate characteristic impedance,

$$Z_0 = \sqrt{Z/Y},$$

obeys. Others [4] choose to classify the line by the functional form exhibited by the distributed immittances themselves. At any rate, the solutions of the general Telegraphers' equations of (1) and (2) are difficult to obtain and usually cannot be handled by analytic

methods forcing recourse to numerical techniques.

Proceeding, then, with the analysis of the problem at hand, it is required to place in emphasis the line characteristics rather than the line voltages and currents that appear in equations (3) and (4). Pierce[9] shows that it is possible to describe the nonuniform transmission line by a first order nonlinear differential equation in impedances only. Walker and Wax[10] followed the same procedure and introduced further a transformation process to determine the resonance behavior of a nonuniform transmission line. Following the procedure of Pierce, the impedance may be expressed as:

$$Z_0 \frac{dZ}{dy} = \gamma (Z_0^{\,2} - Z^2), \tag{5}$$

where: $Z_0(y)$ is the characteristic (or intrinsic) transmission line impedance,
$Z(y)$ is the impedance variation on the line, and
$\gamma(y)$ is the propagation constant,

with the independent variable y measured from the receiving end. For the purposes of this report, let us locate the origin at the sending end by setting $y = L-x$ where L is the physical length of the line. Upon substitution:

$$Z_0(x) \frac{dZ}{dx} = \gamma (Z^2 - Z_0^{\,2}). \tag{6}$$

Following the usual convention[9,10,11,12], these transformations are introduced:

$$\rho(x) = \frac{Z(x)-Z_0(x)}{Z(x)+Z_0(x)}; \; Z(x) = Z_0(x) \frac{1+\rho(x)}{1-\rho(x)},$$

where $\rho(x)$ is the reflection coefficient. Upon substitution in equation (6), there results the basic differential equation governing the reflection coefficient:

$$\frac{d\rho}{dx} - 2\gamma\rho + \frac{(1-\rho^2)}{2} \frac{d}{dx}(\ln Z_0) = 0. \tag{7}$$

This expression is a first order nonlinear differential equation with variable coefficients known as "Riccati's Equation." As it stands, the equation is exact, the only assumption underlying its derivation being the requirement for the existence of the TEM mode. With this expression it is possible, at least in principle, to determine the reflection coefficient anywhere on the nonuniform transmission line once the distributed series impedance function and distributed shunt admittance function are specified (using $\gamma = \sqrt{ZY}$, $Z_0 = \sqrt{Z/Y}$).

In the problem of matching the characteristic impedances of two uniform transmission lines with a section of nonuniform transmission line (taper), it is obvious that the transformer must satisfy the paramount design criterion - the insertion mismatch due to the nonuniform section be as small as possible. As such, it is reasonable to assume that the reflection coefficient will be much smaller than unity everywhere in the nonuniform line. Thus, if

$|\rho(x)|^2 << 1$, then equation (7) becomes:

$$\frac{d\rho}{dx} - 2\,\gamma\rho + \frac{1}{2}\frac{d}{dx}(\ln Z_0) = 0. \tag{8}$$

The equation is now linearized and a solution easily available. The details of the solution are given in the appendix with the following results:

$$\rho(x) = \rho(L)\exp\left[-2\int_x^L \gamma(\xi)\,d\xi\right] + \frac{1}{2}\exp\left[2\int_{x_0}^{x}\gamma(\xi)\,d\xi\right]\left\{\int_x^L \frac{d}{dt}[\ln Z_0(t)]\exp\left[-2\int_{t_0}^{t}\gamma(\xi)\,d\xi\right]dt\right\}. \tag{9}$$

Although this appears as a formidable practical solution, it lends itself to further simplification. Let us consider x_0 as the origin of the coordinate system and assume that the nominal propagation constant is pure imaginary and not a function of the independent variable x. The latter assumption essentially means a lossless, nondispersive transmission line thus excluding tapered dielectric media, hollow wave guides, etc. Thus, if $x_0 = 0$ $(t_0 = 0)$ and $\gamma(x) = jB$, then equation (9) becomes:

$$\rho(x) = \rho(L)\,e^{j2\beta(x-L)} + \frac{1}{2}e^{j2\beta x}\int_x^L \frac{d}{dt}[\ln Z_0(t)]\,e^{-j2\beta t}\,dt.$$

Now, if in addition, the line is assumed perfectly matched at the receiving end, $\rho(L) = 0$, the reflection coefficient at the sending end $\rho(0)$ is simply:

$$\rho(0) = \frac{1}{2}\int_0^L \frac{d}{dx}[\ln Z_0(x)]\,e^{-j2\beta x}dx. \tag{10}$$

III. THE COSINUSOIDAL TAPERED TRANSFORMER

The problem now is to match two transmission lines of characteristic impedance of Z_{01} and Z_{02} respectively by the insertion of a suitable section of nonuniform transmission line, that is, a taper. In consonance with the above theory, it is assumed that both lines are either infinite in extent or perfectly matched in their own characteristic impedances. The TEM wave in the sending line propagates without reflections into the nonuniform section and then undergoes continuous reflections for the whole of this path. Upon emerging, the wave progresses again without reflections and is finally totally absorbed in the receiving termination. Of course, while the wave train is propagating in the uniform sending line, it combines in a standing wave with the composite reflected wave from the integrated finite (but small) discontinuity that appears at the input plane to the transformer.

Figure 1 shows the physical arrangement being considered together with the impedance distribution chosen. The mathematical description of the arrangement is:

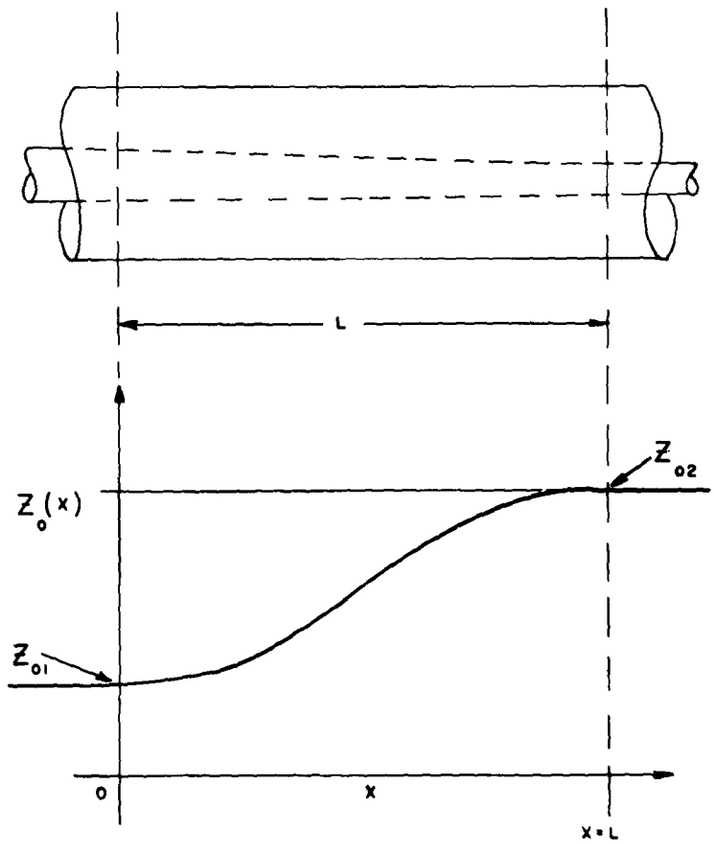

Figure 1. Taper Contour and Impedance Distribution.

$$Z_0(x) = Z_{01}, \quad x \leq 0,$$

$$Z_0(0) = Z_{02}, \quad x \geq L,$$

and

$$Z_0(x) = \frac{Z_{01} + Z_{02}}{2} + \frac{Z_{01} - Z_{02}}{2} \cos \frac{\pi x}{L}, \quad 0 \leq x \leq L.$$

Note that the cosinusoidal distribution satisfies the boundary conditions, is continuously differentiable, and physically realizable. To calculate the input reflection at $x = 0$ using equation (10), proceed as follows:

$$\frac{d}{dx}[\ln Z_0(x)] = \frac{d}{dx} \ln \left[\frac{Z_{01} + Z_{02}}{2} + \frac{Z_{01} - Z_{02}}{2} \cos \frac{\pi x}{L}\right]$$

$$= \frac{\left(\frac{Z_{02} - Z_{01}}{2}\right) \frac{\pi}{L} \sin \frac{\pi x}{L}}{\frac{Z_{01} + Z_{02}}{2} + \frac{Z_{01} - Z_{02}}{2} \cos \frac{\pi x}{L}},$$

and upon simplification,

$$\frac{d}{dx}\ln Z_0(x) = \frac{\frac{\pi}{L}\sin\frac{\pi x}{L}}{\left(\frac{Z_{01}+Z_{02}}{Z_{02}-Z_{01}}\right) - \cos\frac{\pi x}{L}} . \tag{11}$$

Now, define the unmatched reflection coefficient (pure real due to the terminating requirements assumed previously) as:

$$\rho_0 = \frac{Z_{02} - Z_{01}}{Z_{02} + Z_{01}} .$$

Equation (11) then becomes:

$$\frac{d}{dx}\ln Z_0(x) = \frac{\rho_0\pi}{L}\,\frac{\sin\frac{\pi x}{L}}{\left(1 - \rho_0\cos\frac{\pi x}{L}\right)},$$

and upon substitution in the expression for input reflection coefficient,

$$\rho(0) = \frac{\rho_0\,\pi}{2L}\int_0^L \frac{\sin\frac{\pi x}{L}}{\left(1-\rho_0\cos\frac{\pi x}{L}\right)}\, e^{-j2\beta x}\, dx. \tag{12}$$

Changing variables according to $\pi x/L \to \theta$,

$$\frac{\rho(0)}{\rho_0} = \frac{1}{2}\int_0^{\pi} \frac{\sin\theta}{1-\rho_0\cos\theta}\, e^{-j\frac{4L}{\lambda_0}\theta}\, d\theta, \tag{13}$$

where λ_0 is the free space wavelength. Expanding (13)

$$\frac{\rho(0)}{\rho_0} = \frac{1}{2}\left\{\int_0^{\pi} \frac{\sin\theta\cos\frac{4L}{\lambda_0}\theta}{1-\rho_0\cos\theta}\, d\theta - j\int_0^{\pi} \frac{\sin\theta\sin\frac{4L}{\lambda_0}\theta}{1-\rho_0\cos\theta}\, d\theta\right\}.$$

Finally, the magnitude of the normalized input reflection coefficient is:

$$\left|\frac{\rho(0)}{\rho_0}\right| = \frac{1}{2}\left\{\left[\int_0^{\pi} \frac{\sin\theta\cos\frac{4L}{\lambda_0}\theta}{1-\rho_0\cos\theta}\, d\theta\right]^2 + \left[\int_0^{\pi} \frac{\sin\theta\cos\frac{4L}{\lambda_0}\theta}{1-\rho_0\cos\theta}\, d\theta\right]^2\right\}^{1/2}. \tag{14}$$

The above expression cannot be integrated analytically (in closed form) except for certain discrete values of the parameters L/λ_0 and ρ_0. To obtain engineering design curves based on equation (14), it is required to evaluate the above over the significant range of parameters in the integral arguments. In this way, there evolves a family of curves giving the normalized input reflection coefficient as a function of the electrical length L/λ_0 with the unmatched reflection coefficient ρ_0 as a design parameter. The above integrals were evaluated utilizing a numerical integration method known as the Gaussian Quadrature

technique. The actual computations were performed on a Burrough's Datatron 205 digital computer with the electrical length varying between 3.0 and zero, and the unmatched reflection coefficient varying between 1.0 and zero ($0 < \rho < 1$) both in steps of 0.1. From this machine tabulated data, five graphs of input reflection coefficient as a function of electrical length were constructed for five different values of mismatch as shown in Figures 2-6 and Figures 7-11. For values of mismatch other than those covered by the above iterations, the tabulated data easily permits interpolation to specific cases.

Figure 2. The Magnitude of the Normalized Reflection Coefficient versus the Ratio, Physical Length/Wavelength for $\rho_0 = 0.1$.

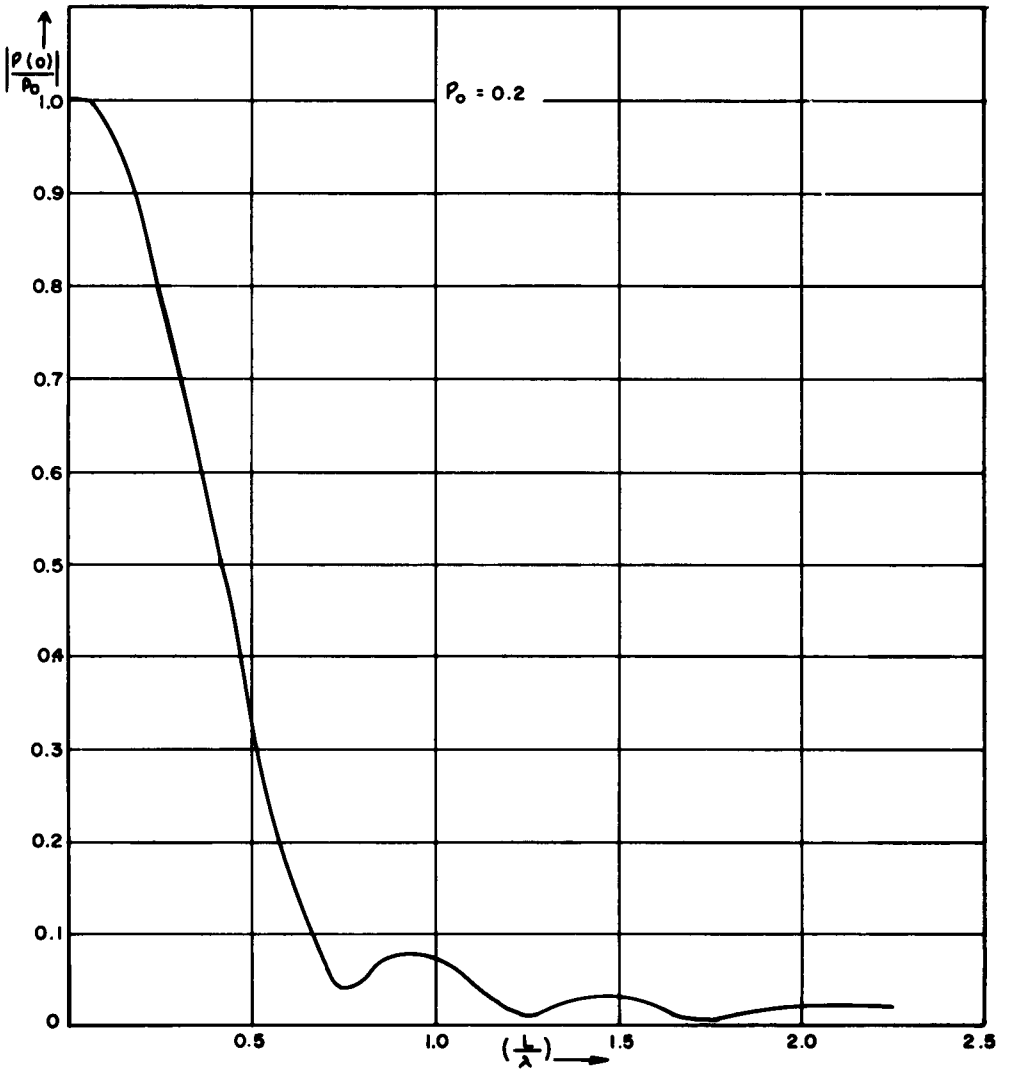

Figure 3. The Magnitude of the Normalized Reflection Coefficient versus the Ratio, Physical Length/Wavelength for $\rho_0 = 0.2$.

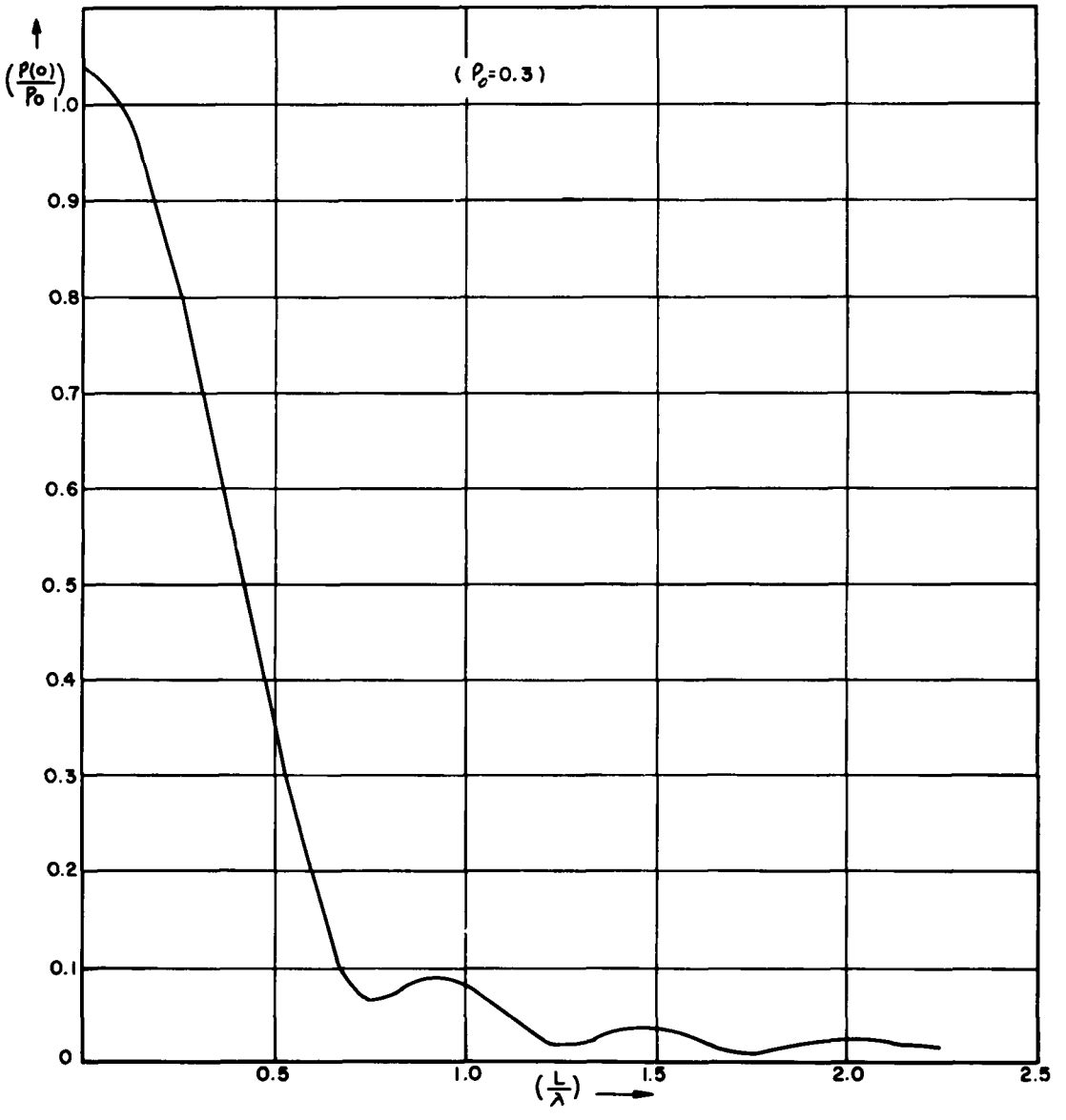

Figure 4. The Magnitude of the Normalized Reflection Coefficient versus the Ratio, Physical Length/Wavelength for ρ_0 = 0.3.

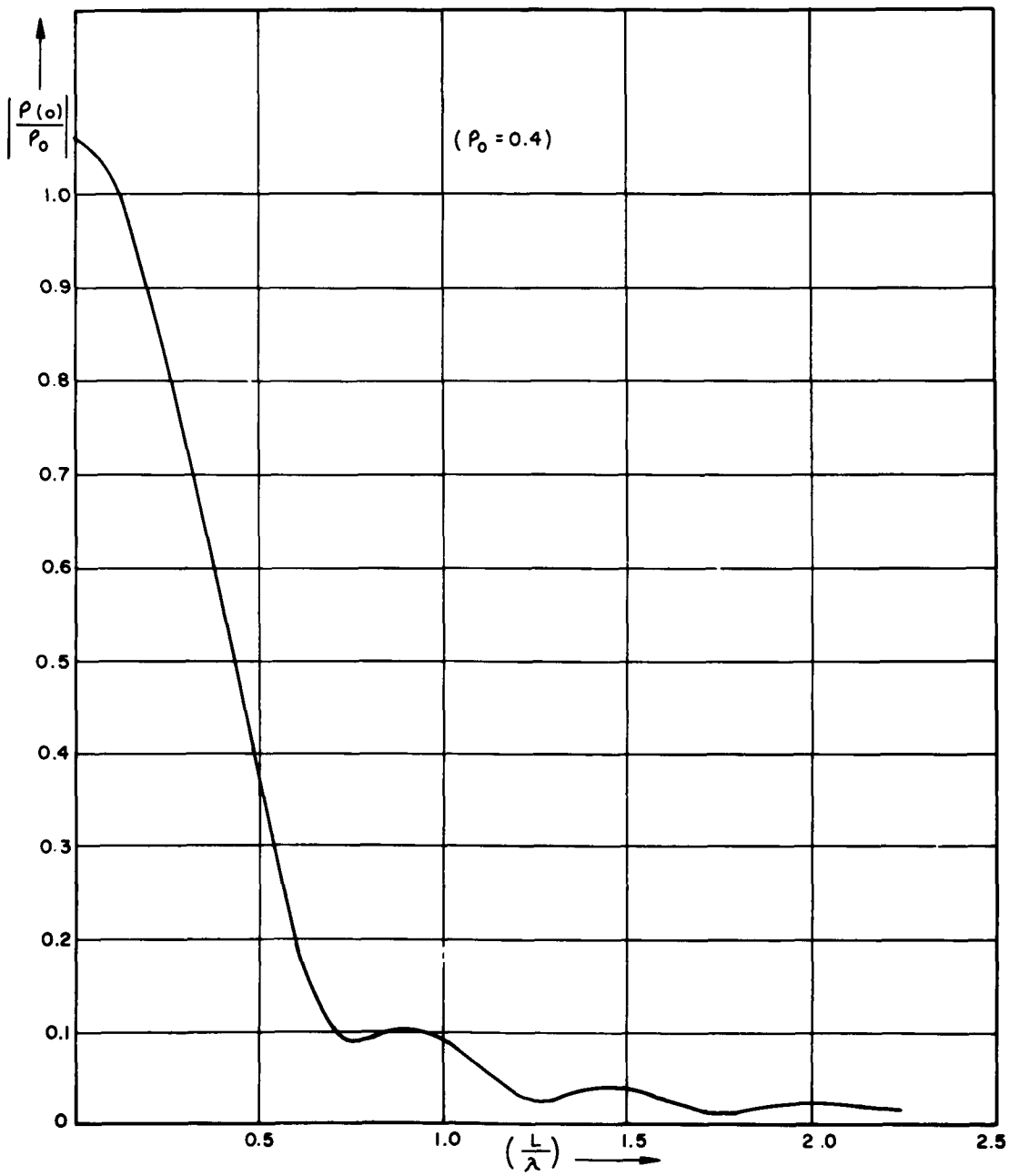

Figure 5. The Magnitude of the Normalized Reflection Coefficient versus the Ratio, Physical Length/Wavelength for $\rho_0 = 0.4$.

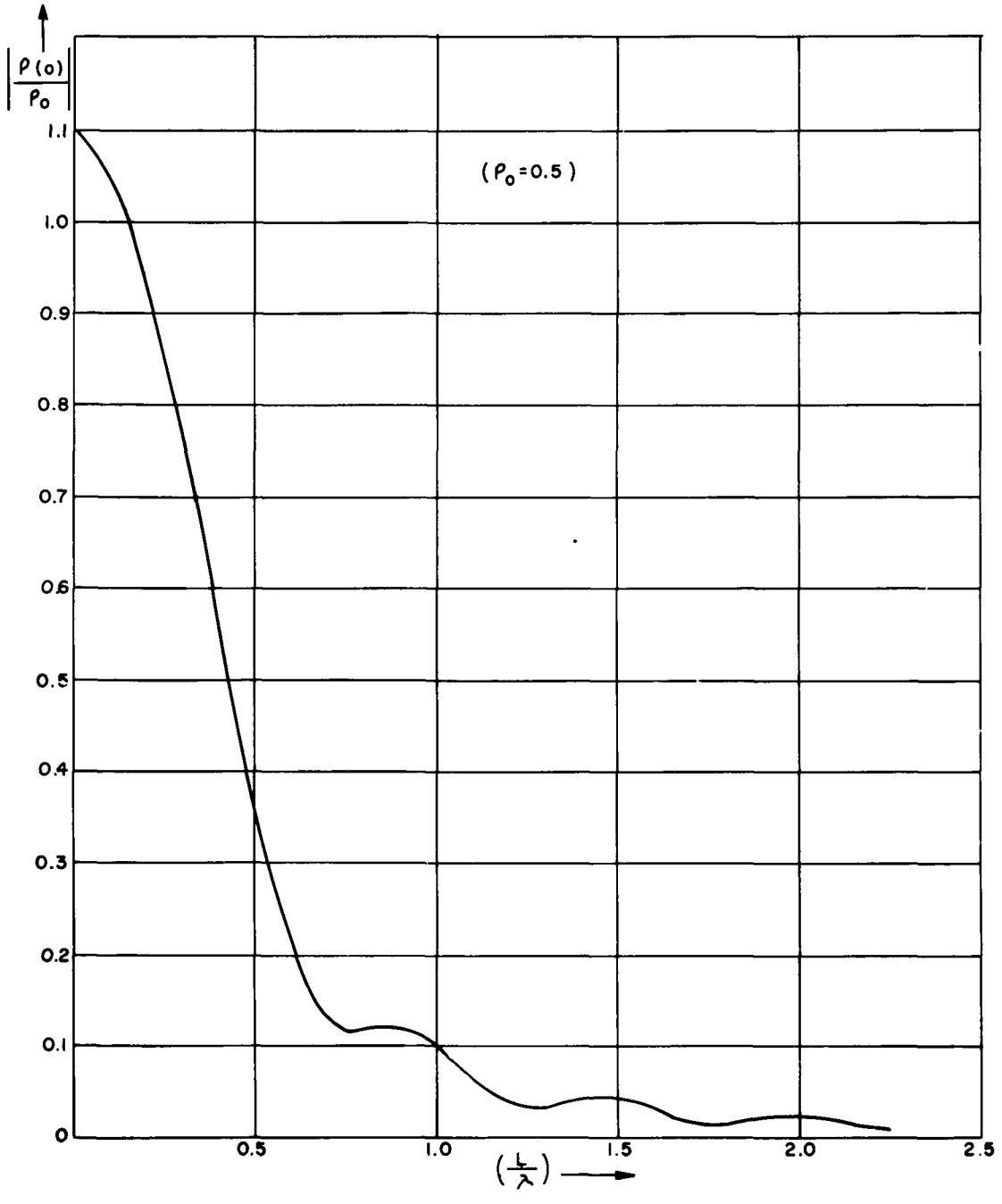

Figure 6. The Magnitude of the Normalized Reflection Coefficient versus the Ratio, Physical Length/Wavelength for $\rho_0 = 0.5$.

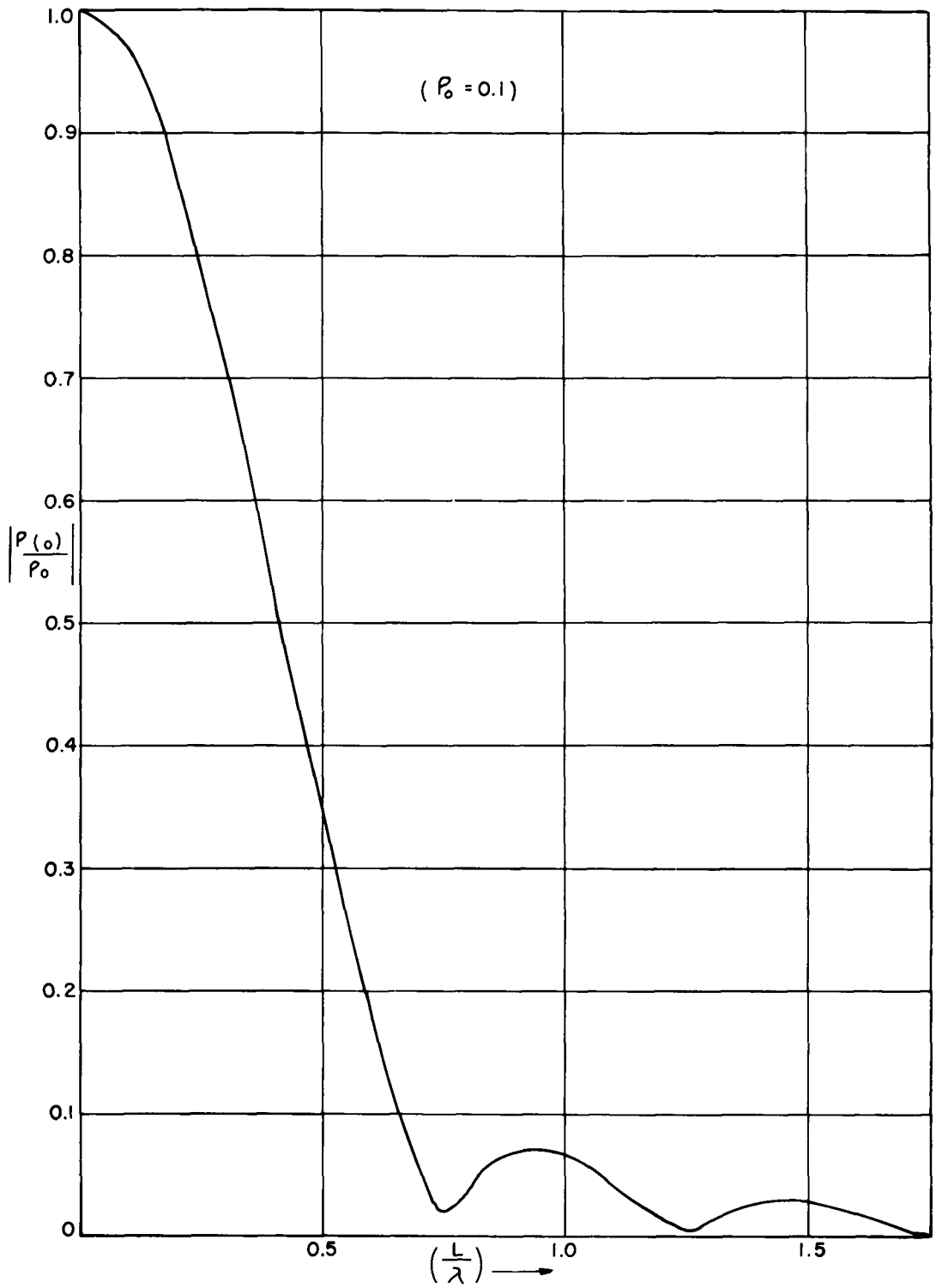

Figure 7. Figure 2 Renormalized with the Consistent ρ_0.

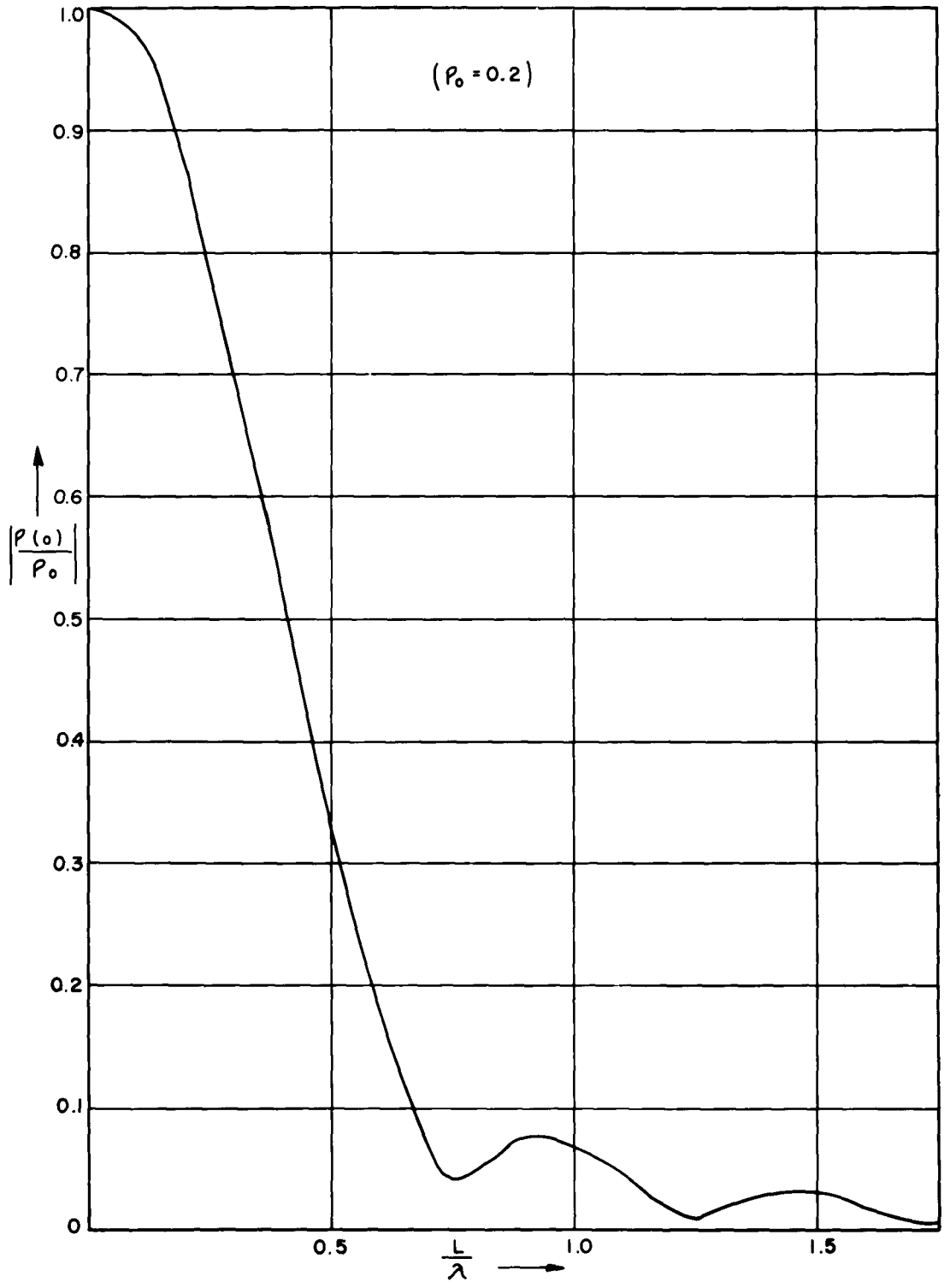

Figure 8. Figure 3 Renormalized with the Consistent ρ_0.

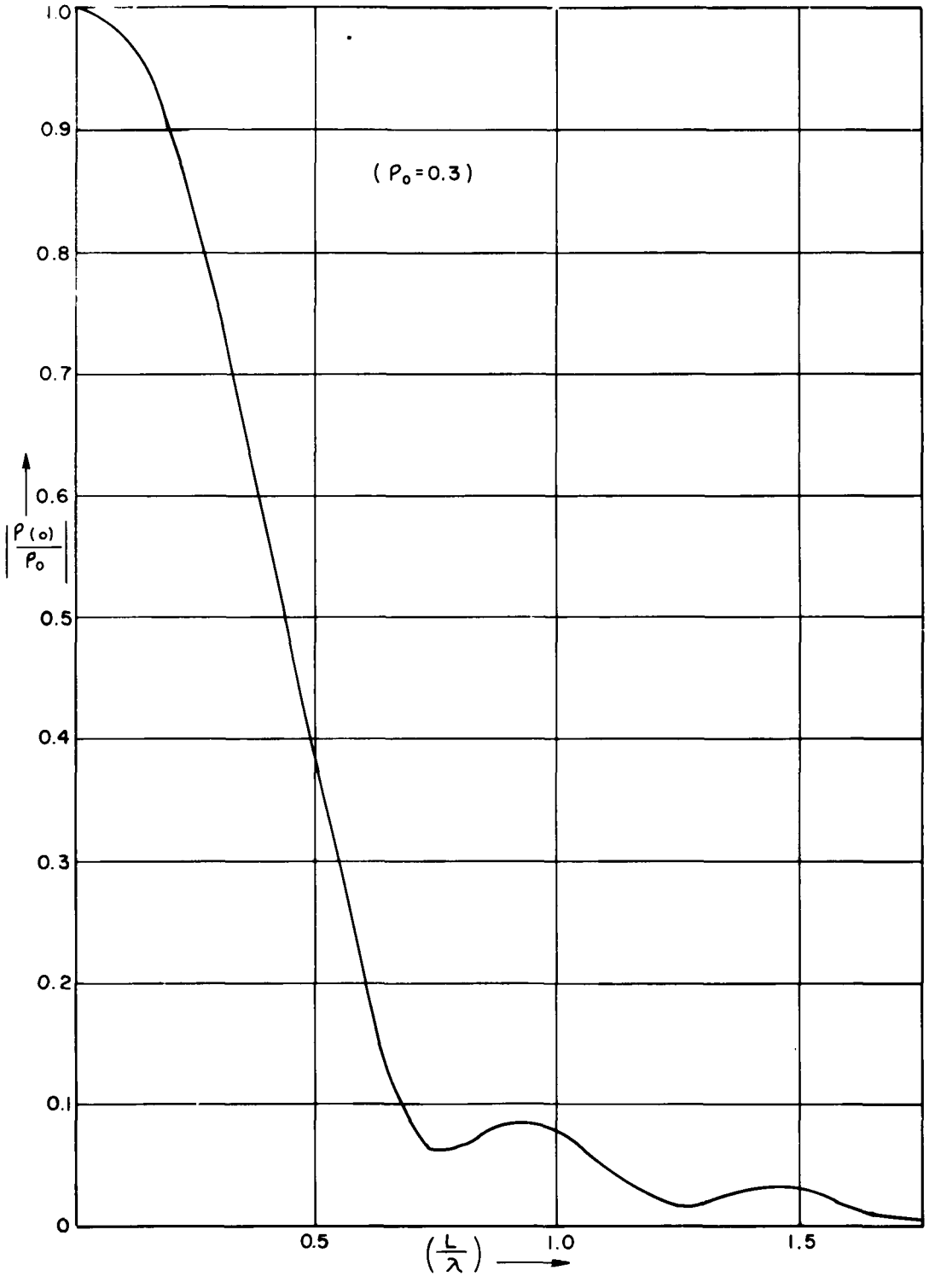

Figure 9. Figure 4 Renormalized with the Consistent ρ_0.

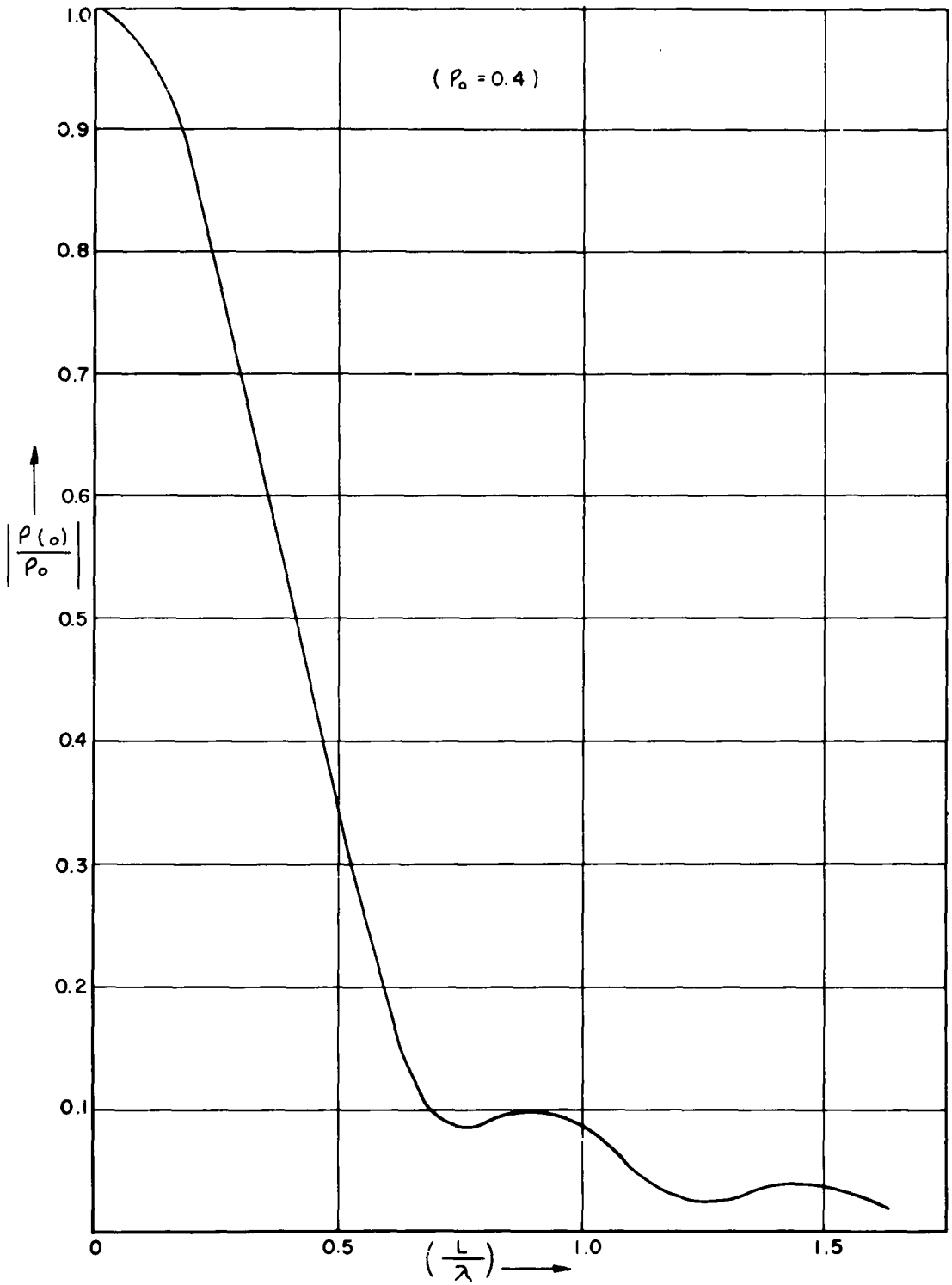

Figure 10. Figure 5 Renormalized with the Consistent ρ_0.

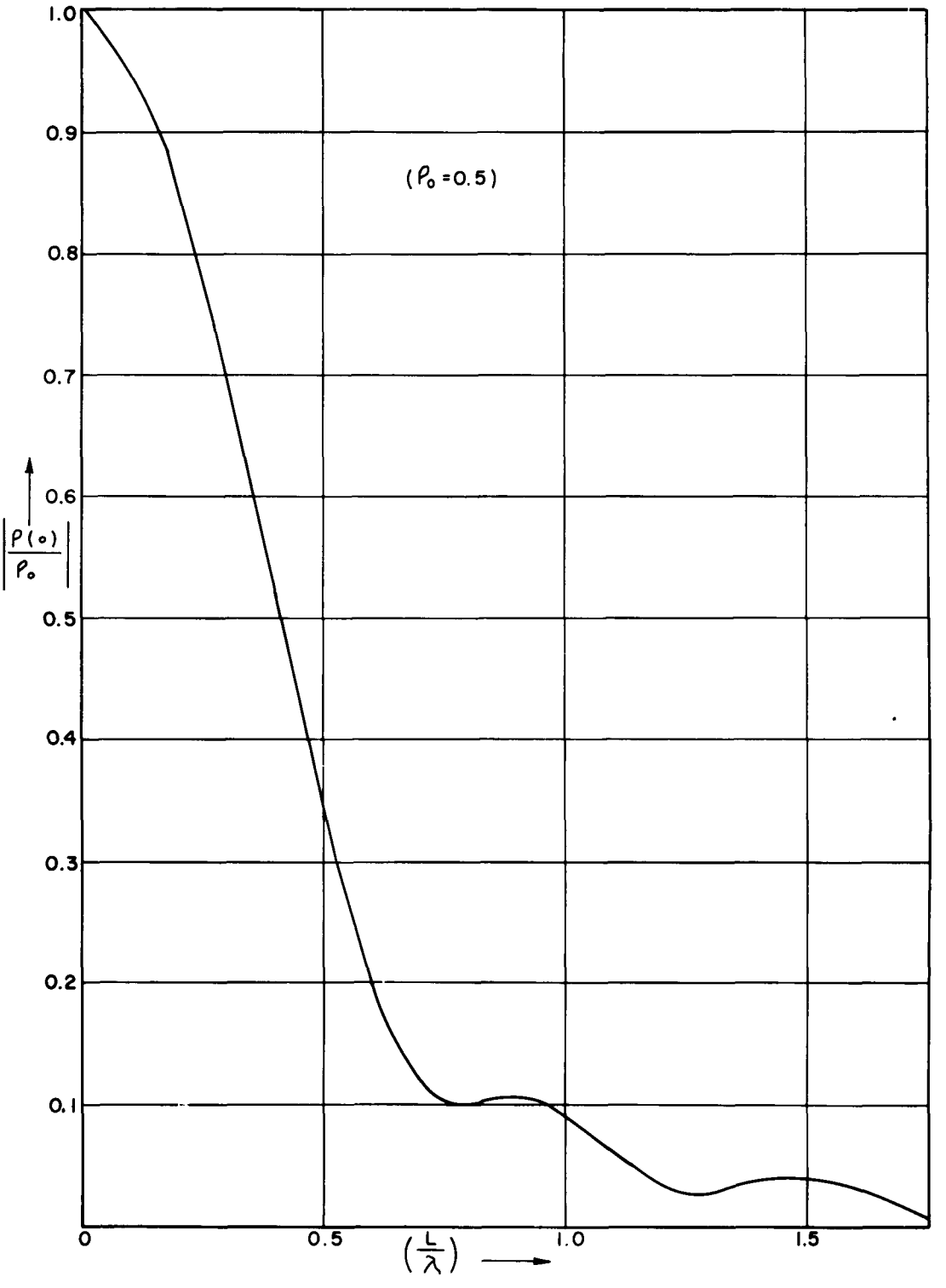

Figure 11. Figure 6 Renormalized with the Consistent ρ_0.

IV. THEORETICAL RESULTS

Close examination of the predicted performances of the cosinusoidal transformer indicates some interesting characteristics. The most prominent feature, and somewhat embarrassing, are the curves (Figures 2-6) that show normalized reflection coefficients exceeding unity for (L/λ_0) equal to zero. The normalizing parameter ρ_0 was previously defined as the mismatched reflection coefficient - namely, the input reflection coefficient without a transformer. Thus, for $L \to 0$, $\lambda_0 \to \infty$ the input reflection coefficient $\rho(0)$ is self-normalized, $\rho(0) \equiv \rho_0$, and cannot exceed unity. The fact that the computed results indicate the contrary may be explained quantitatively as follows. Recalling the generalized statement for the input reflection coefficient derived previously as equation (10):

$$\rho(0) = \frac{1}{2} \int_0^L \frac{d}{dx} [\ln Z_0(x)]\, e^{-j2\beta x}\, dx,$$

it can be shown[8] that as $L \to 0$ as a limit, or alternatively as $\beta \to 0$ $(\lambda_0 \to \infty)$, the above expression approaches:

$$\rho(0) \to \frac{1}{2} \ln \frac{Z_0(L)}{Z_0(0)} .$$

Namely, the input reflection coefficient becomes proportional to the natural logarithm of the ratio of the end point characteristic impedances (!) regardless of the explicit functional form of $Z_0(x)$. Thus, the mathematically consistent normalizing parameter should be:

$$\rho(0) = \frac{1}{2} \ln \frac{Z_0(L)}{Z_0(0)} = \rho_0 .$$

Now, for the particular nonuniform impedance distribution - the cosinusoidal function - the normalizing parameter assumed intuitively was:

$$\rho_0 = \frac{Z_0(L) - Z_0(0)}{Z_0(L) + Z_0(0)} ,$$

or simply the well-known reflection coefficient for a step discontinuity. Although this is exact, its use in the linearized theory of nonuniformly distributed matching sections will lead to the above theoretical inconsistency. The error introduced by the choice of the consistent normalization parameter instead of the exact one has been computed elsewhere[13] to be less than:

$$\frac{1}{24}\left[\frac{Z_0(L) - Z_0(0)}{Z_0(0)}\right]^3$$

Thus, for small values of mismatched reflection coefficients, $Z_0(L) \doteq Z_0(0)$, the error is insignificant but becomes prominent for large mismatches. The curves of Figures 2-6 vividly demonstrate this fact.

In the preceding explanation for the anomalies in the normalized reflection coefficients for L/λ_0 equal to zero, it was tacitly assumed that equation (10) is valid on the closed interval $[0, L]$, thus allowing an essentially mathematical argument. Although questionable on other grounds, it is a reasonable assumption because the Burrough's Datatron 205 computer which generated the theoretical data for the cosinusoidal distribution did so gullibly obeying its program with the same inherent assumption. Now, allowing $(L/\lambda_0) \to 0$ in the physical sense means that the period of the cosinusoidal variation is decreasing or that the transformer is literally shrinking up.

The physical significance of this contraction implies an increasingly more violent taper, the slope of which is approaching that of a stepped discontinuity. It is obvious that in such a case the magnitude of the reflection coefficient in the cosinusoidal section will become appreciable, thus violating the linearizing condition on the Riccati differential equation. In other words, equation (10) represents the solution to the linearized Riccati equation subject to the condition requiring $|\rho(x)|^2 << 1$ throughout the nonuniform section. Consequently, the normalized reflection coefficient curves in Figures 2-6 (and Figures 7-11) are in serious doubt when $(L/\lambda_0) \to 0$. However, from the point of view of engineering high quality impedance matching transformers, that region of these design curves is mainly of academic interest.

The discrepancies inherent in Figures 2-6 are pointed out and discussed mainly for the purposes of signifying a possible strategic pitfall in the linearization process of the Riccati equation and the erroneous engineering value in the use of the subsequent results. Consequently, Figures 2-6 were corrected with respect to the mathematically consistent normalization parameter and are given in Figures 7-11. The most important aspect of these theoretical data for the cosinusoidal transition is observed in the design curves of Figures 7-11. A critical examination of these predicted results in comparison to the predictions of other distributions reported in the literature indicates that the cosinusoidal variation offers significant improvement in over-all performance. In the Dolph-Tchebycheff tapered transition [14] for a 50-75 ohm impedance mismatch, it is observed that side lobes of the bandpass curves are of equal height with a normalized reflection coefficient of approximately 0.0537.

The minimums occur at approximately 0.637 L/λ_0, 0.955 L/λ_0, 1.364 L/λ_0, 1.817 L/λ_0, etc. A comparison of these data with Figure 8 of this report shows that the Dolph-Tchebycheff first side lobe is approximately 28 percent less than the cosinusoidal first lobe, but the cosinusoidal second lobe is approximately 44 percent less than the Dolph-Tchebycheff case. Thus, for this particular mismatch (50-75 Ω), the cosinusoidal

distribution offers considerable improvement of ripple in the passband providing that the frequency and length are chosen such that $(L/\lambda_0) > 1.125$ is always satisfied.

The exponential taper for the same mismatch conditions, 50-75 Ω exhibits[14] approximate peaks in the normalized reflection coefficient side lobes as follows: first, - 0.214, second - 0.125, third - 0.089, etc. Comparison of these data with Figure 8 indicates much superior performance for the cosinusoidal distribution. In fact, the latter does not exhibit the highest exponential peak until L/λ_0 is about 0.575, while the exponential distribution gives this value for L/λ_0 of approximately 0.682. In other words, if a normalized reflection coefficient of 0.214 is the acceptable maximum, then the cosinusoidal-transformers offer an approximately 16 percent greater bandwidth over an exponential transformer of the same physical length, or alternately for the same bandwidths, a 16 percent reduction in pysical size.

The hyperbolic taper[15] for the same mismatched conditions exhibits no side lobes, but rather a monotonically decreasing normalized reflection coefficient for increasing L/λ_0. The cosinusoidal transformer when compared to this distribution is drastically superior. For example, if a normalized reflection coefficient of 0.1 is the acceptable maximum, then Figure 8 indicates that the cosinusoidal transformer will satisfy the requirement with $L/\lambda_0 > 0.67$. The hyperbolic transformer, on the other hand, demands an L/λ_0 equal to or in excess of about 1.41. In other words, for the same lengths of line, the cosinusoidal transformer offers approximately a 53 percent improvement in acceptable bandwidth over the hyperbolic design. Alternatively, for a common fixed bandwidth, the cosinusoidal design will satisfy the requirements in roughly half the physical size of the hyperbolic transformer.

V. EXPERIMENTAL ANALYSIS

To authenticate the theoretical results embodied in Figures 7-11, an experimental demonstration was conceived and designed to corroborate the theoretical predictions. Since one author[15] presented a comparison of theoretical performance of several kinds of taper distributions for a 50-150 ohm mismatch, it was decided to use this mismatch as the comparative criterion. Figure 12 shows the pertinent theoretical data for the hyperbolic, exponential, and Bessel sections together with the cosinusoidal performance from Figure 11 for this particular case. Again, the cosinusoidal transformer seems to be the superior one.

The large side lobes in the exponential and Bessel sections compared to those of the cosinusoidal section are their main drawbacks, while the slowly changing slope of the hyperbolic section (at the expense of bandwidth or physical size) is its main drawback. The test vehicle objective will then be to design and experimentally test a transformer for a mismatch condition of 0.5, which corresponds to a 50-150 ohm transition. In this way, a direct comparison with Figure 11 (and 12) may be made. Furthermore, the available microwave instrumentation in the nominal 50 ohm characteristic impedance lends itself readily to the uniform sending end of the transformer.

The actual design of the transformer proceeds quite easily. From the significant range

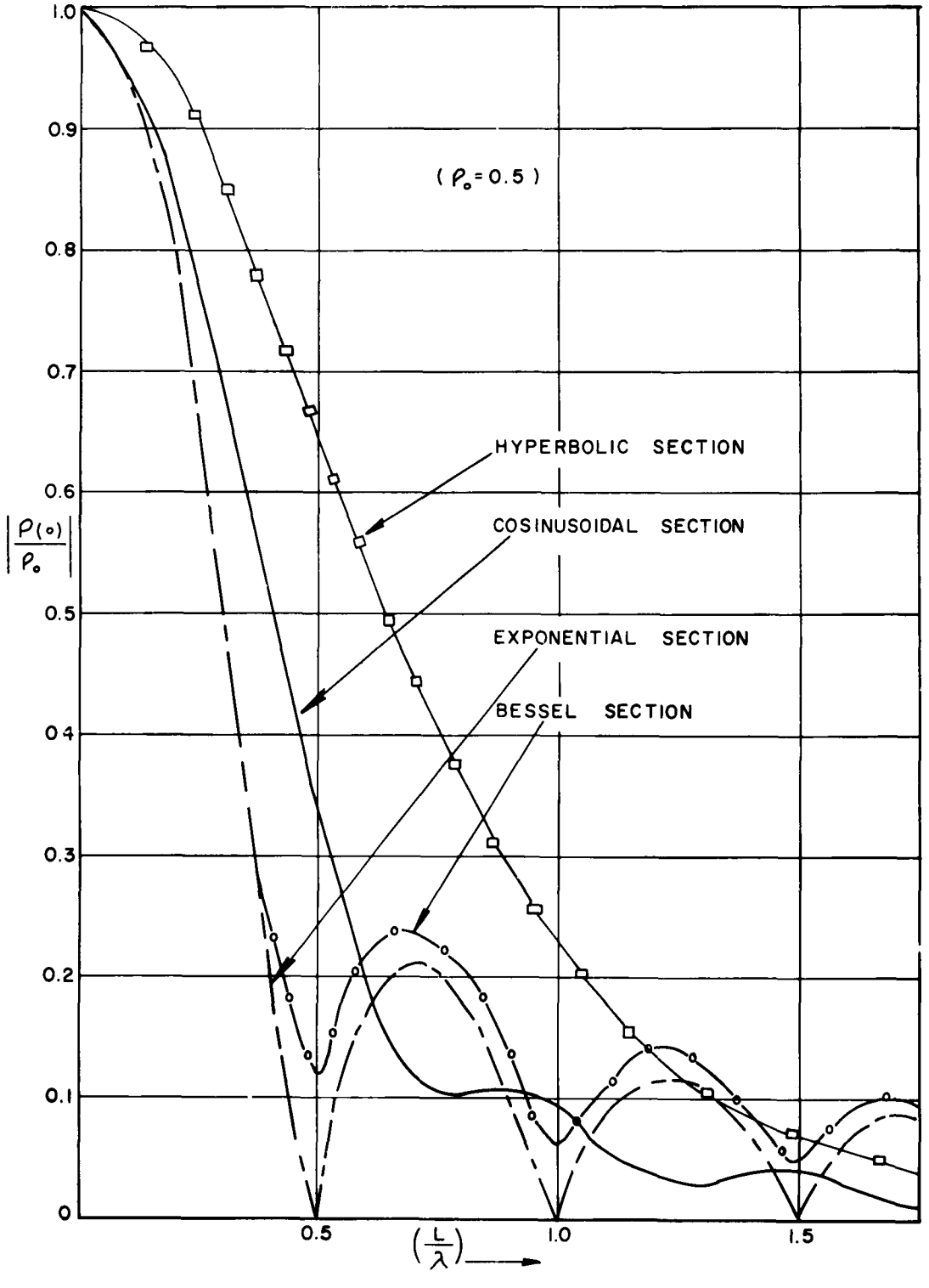

Figure 12. Comparative Transformer Performance for a 50 percent Mismatch.

of the parameter L/λ_0, the physical length of the transformer is fixed so as to exhibit a bandwidth that encompasses the essential highlights of Figure 11. For the case treated this length comes out to be about 23 cm. With the end point characteristic impedances specified as 50Ω and 150Ω, respectively, the appropriate cosinusoidal distribution becomes:

$$Z_0(x) = \frac{Z_{01} + Z_{02}}{2} + \frac{Z_{01} - Z_{02}}{2} \cos \frac{\pi x}{L},$$

or

$$Z_0(x) = 100 - 50 \cos \frac{\pi x}{23} \; (x \text{ in cm}).$$

To realize this distribution, the inner conductor of a coaxial section is machine tapered to give a variable radius satisfying $Z_0 = 60 \ln \frac{R_0}{r_i}$, where R_0 is the inner radius of the outer conductor and r_i the outer radius of the inner conductor. Thus, the physical profile of the variation in the inner conductor obeys:

$$r_i(x) = R_0 \exp \left[- \frac{1}{60} \left(100 - 50 \cos \frac{\pi x}{L}\right)\right] \; (x \text{ in cm}).$$

The choice of line size is dictated by the availability of test instrumentation in various line sizes, and also by what is physically practical at the receiving or terminating end of the transformer. For example, the choice of standard 3/8 inch coaxial line for the sending end would result in a receiving coaxial line, whose inner conductor would be prohibitively small from the mechanical tolerance and fragility aspects. Based on the above considerations, it was decided to use standard 7/8 inch rigid coaxial line, which results in a receiving line whose inner conductor is slightly less than 1/8 inch in diameter. The finished unit with the outer conductor removed is shown in Figure 13a.

Two sections were constructed with male and female end connectors using silver plated solid brass throughout. The tapered profiles were realized from standard bar stock of 3/8 inch diameter by first machine cutting a "staircase" distribution which represents an outside approximation to the taper profile. Figure 13b shows the engineering drawing used to determine the steps' height and length. At the indicated stations the staircase fit is exact within the appropriate tolerances. With these tolerances satisfied at the beginning and end of each step throughout the transformer, the individual step corners were then finished down by hand filing. Finally, a smooth gradual transition was effected by hand rubbing with #400 emery paper followed by silver electroplating and polishing.

Now, in the derivation of the input reflection coefficient for this transformer, it will be recalled that the receiving line must be terminated in a reflectionless load. Unfortunately, broadband (500 mc - 4 kmc) 150 ohm terminations in this unconventional line size are not available without the expenditure of considerable design effort. Nevertheless, a modest amount of effort was expended in an attempt to realize a suitable broadband (100 mc/s to 4 kmc/s) termination. The technique involves the use of a thin conducting film placed at a quarter wavelength from the metallic surface of an ideal short circuit in the

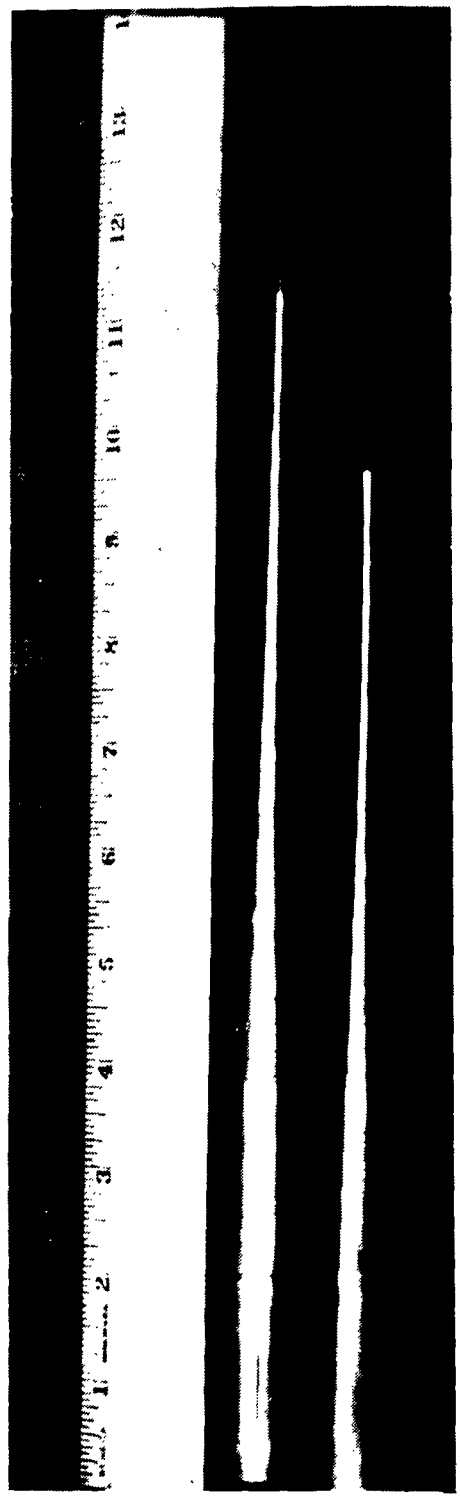

Figure 13a. Photograph of the Inner Conductor of the Cosinusoidal Transformer.

150 ohm transmission line. Consider a thin coaxial film of a good metallic conductor with a large shunt conductance and a negligible shunt capacitance (that is, $\sigma >> \omega \epsilon$), separated by a quarter wavelength from a highly conducting sliding piston. This 150 ohm sliding short will provide the tunability of the termination.

For a quarter wavelength separation the film is at a point of maximum electric field and maximum attenuation. In fact, the combination of film and short will be a perfectly matched[16] load provided that $(\alpha d)^2 << 1$ and $(\beta d)^2 << 1$, where α and β are the attenuation and phase constants, respectively, of the metal film and d the thickness. Now, for a good conductor, the attenuation and phase factors are both equal to the reciprocal skin depth and $\pi/4$ radians out of phase. For these conditions the surface resistivity of the film is calculated to be equal to the characteristic impedance of the 150 ohm line with a film thickness much less than the minimal skin depth expected (at the high end of the bandwidth).

With the above design criteria formulated, a search of commercial manufacturers of microwave resistive films revealed one whose product satisfied the specifications. The company is the Filmohm Corporation of 48 West 25th Street, New York, New York, manufacturing two forms of acceptable film material. Both types are available in the requisite 150 ohm per square resistivity using a michrome deposition of 1.27 micron thickness on high temperature fiberglass in one form, and an artificial mica in the other form. Both types use a mica superstratum to complete a scratch-free sandwiched film construction.

Samples of these materials were obtained, die cut, and placed in a two-inch section of 7/8 inch coaxial 150 ohm transmission line designed to serve as a mount for the film resistor. The mount was constructed so as to permit a firm

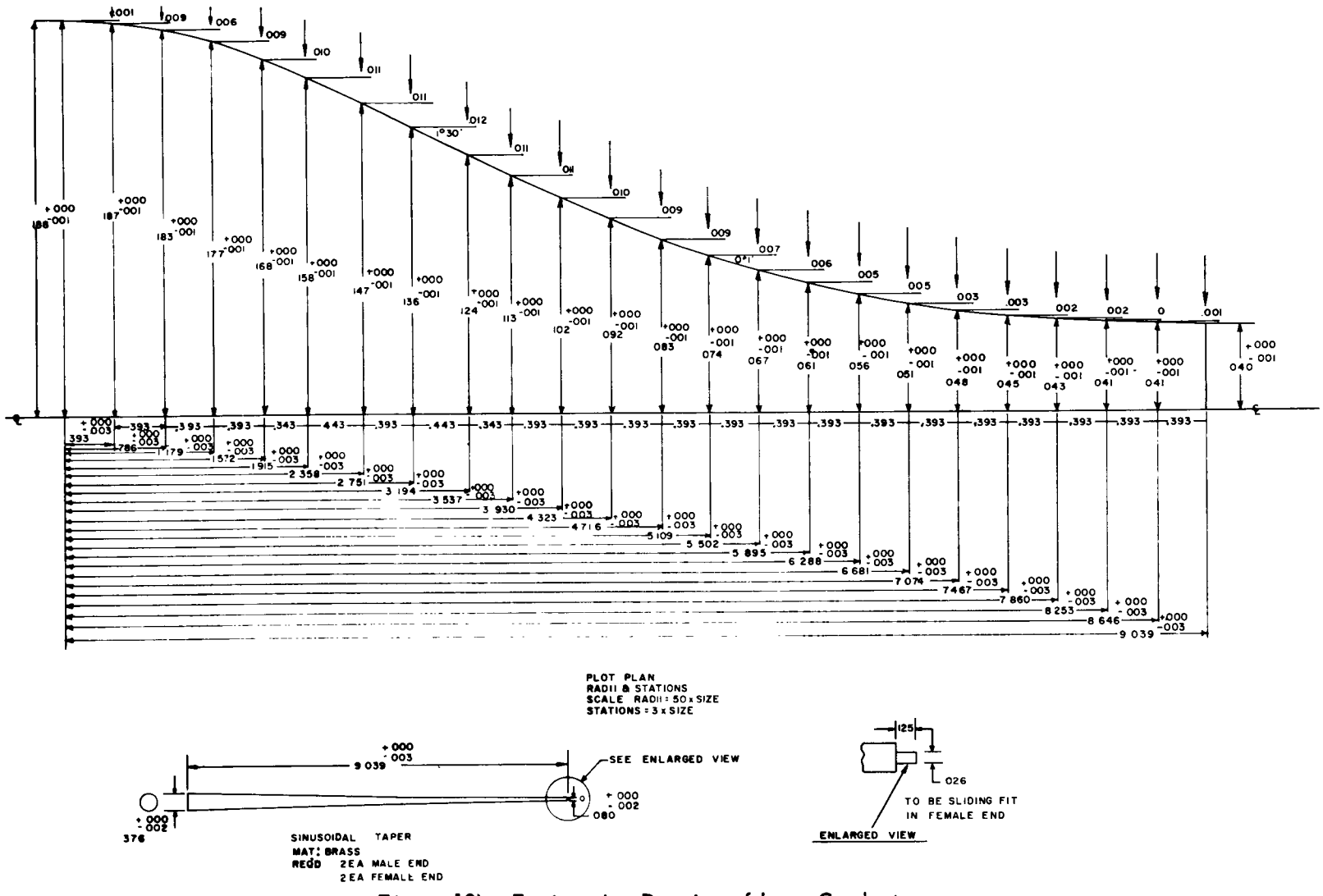

Figure 13b. Engineering Drawing of Inner Conductor.

metal to film pressure fit both at the inner conductor and outer conductor with conductive silver paint (Dupont #4548 or #5584) forming an intermediate layer between coaxial metal and film resistor. Thus, the mount is constructed to guarantee electrical continuity and, at the same time, to provide a rigid mechanical support for the somewhat fragile films. Finally, a sliding short circuit in the 150 ohm transmission line was designed to mate with the output end of the transformer in conjunction with the thin film resistor mount, thereby completing the tunable 150 ohm termination.

This load configuration terminating the output port of the transformer was tested at the midband frequency to determine, at least qualitatively, the success of the load design. In other words, for a quarter wavelength setting of the short circuit, the termination should be matched to the output end of the transformer, and the reflection coefficient (and VSWR) measured in the send line should correlate with the predicted reflection coefficient. The results were completely unsatisfactory. No change in VSWR was found for *any* position of the sliding short. In fact, further tests indicated that the shifts in VSWR minimum in the slotted line were a function of the short setting only and independent of the presence of the film. This was confirmed by actual removal of the film mount section. A lack of d-c continuity between the coaxial metal and film resistor was suspected and later confirmed by microscopic inspection of the film resistor.

The substratum for the vaporized michrome metal is a form of artificial mica with a superstratum of the same mica. Clearly, this sandwich-type construction prohibits a silver paint electrical contact. Although this conclusion is obvious now, it was not at the outset of the termination design. Further effort to engineer this tunable load was consequently abandoned in favor of a measurement technique that does not require a matched load. Specifically, a measurement scheme was used that employs lossless reactances only.

The method is based on a graphical determination of the scattering matrix of a two-port junction and is due to the research of Deschamps[17] and the engineering by Storer, et al.[18] Briefly, the technique is as follows: given; a lossless reciprocal two-port network with unequal port characteristic (or wave) impedances and a variable reactance terminating each of the ports in succession, it is possible uniquely to determine the complex scattering matrix of the junction by successive measurements on the excited port. Obviously, such a complete description of the transformer would more than suffice. It is also clear that the coaxial cosinusoidal transformer in question is indeed reciprocal and lossless and, as such, meets the Deschamps criteria.

The variable reactance is simply a sliding short circuit realizing reactances from open circuit to short circuit with one complete quarter wavelength slide. Furthermore, the scattering parameter of primary interest is $S_{11}(W)$ which by definition is the reflection coefficient at the input plane of reference of the transformer when the output port is terminated in its characteristic impedance. Thus, the determination of $S_{11}(W)$ according to the Deschamps method will suffice. The experimental setup to do this is as shown in Figure 14, where the 150 ohm sliding short circuit was custom-designed in-house and described previously. The actual measurements performed consisted of determining the complex

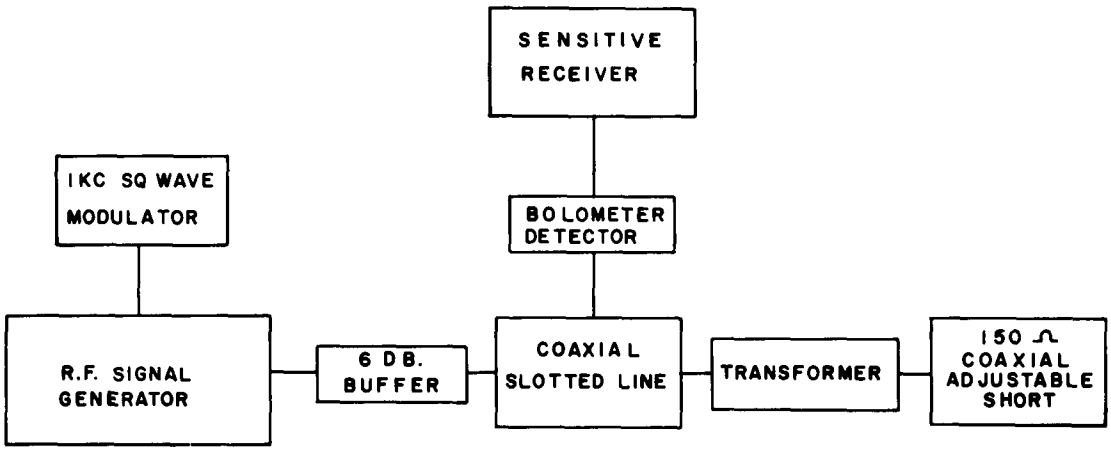

Figure 14. Experimental Block Diagram for the Measurement of the Transformer Scattering Matrix.

input reflection coefficient for four settings of the sliding short circuit spaced about equally over a quarter wavelength. Conventional measurement procedures were employed to determine these reflection coefficients, the results of which were graphically analyzed in accordance with the Deschamps technique.

For the given length of transformer (23 cm) in conjunction with the unmatched 50-150 ohm transition, the theoretical data of Figure 11 were recalculated accordingly, with VSWR versus frequency, and is as shown in Figure 15. The experimental results after graphical analysis are indicated on the same figure by the crosses. As can be readily observed, the correlation is excellent considering the microwave instrumentation employed to determine the input reflection coefficients of the transformer-short circuit combination for the various settings of the adjustable short.

The measurement of the large input standing wave ratios encountered across the whole range of the frequencies of interest requires a highly sensitive bolometer amplifier-detector and a knowledge of the detector response law. The first requirement stems from the need to detect the small signal proportional to the standing wave minimum amplitude in the presence of considerable amplifier noise, and the second requirement dictating the value of the proportionality constant involved. The sensitivity of the instrumentation used was increased considerably by a traveling-wave-tube amplifier between the r-f source and the slotted section. The response curve of the detector was assumed to be square law, that is, the detected output in the region of a standing wave minimum is a quadratic function of probe travel. With this assumption, it is possible to determine the VSWR by examining the region about the minimum. If the distance between points on either side of a minimum with power levels three decibels above the minimum can be determined, and if the distance between two adjacent minima is known, the VSWR can be obtained from the relationship:[19]

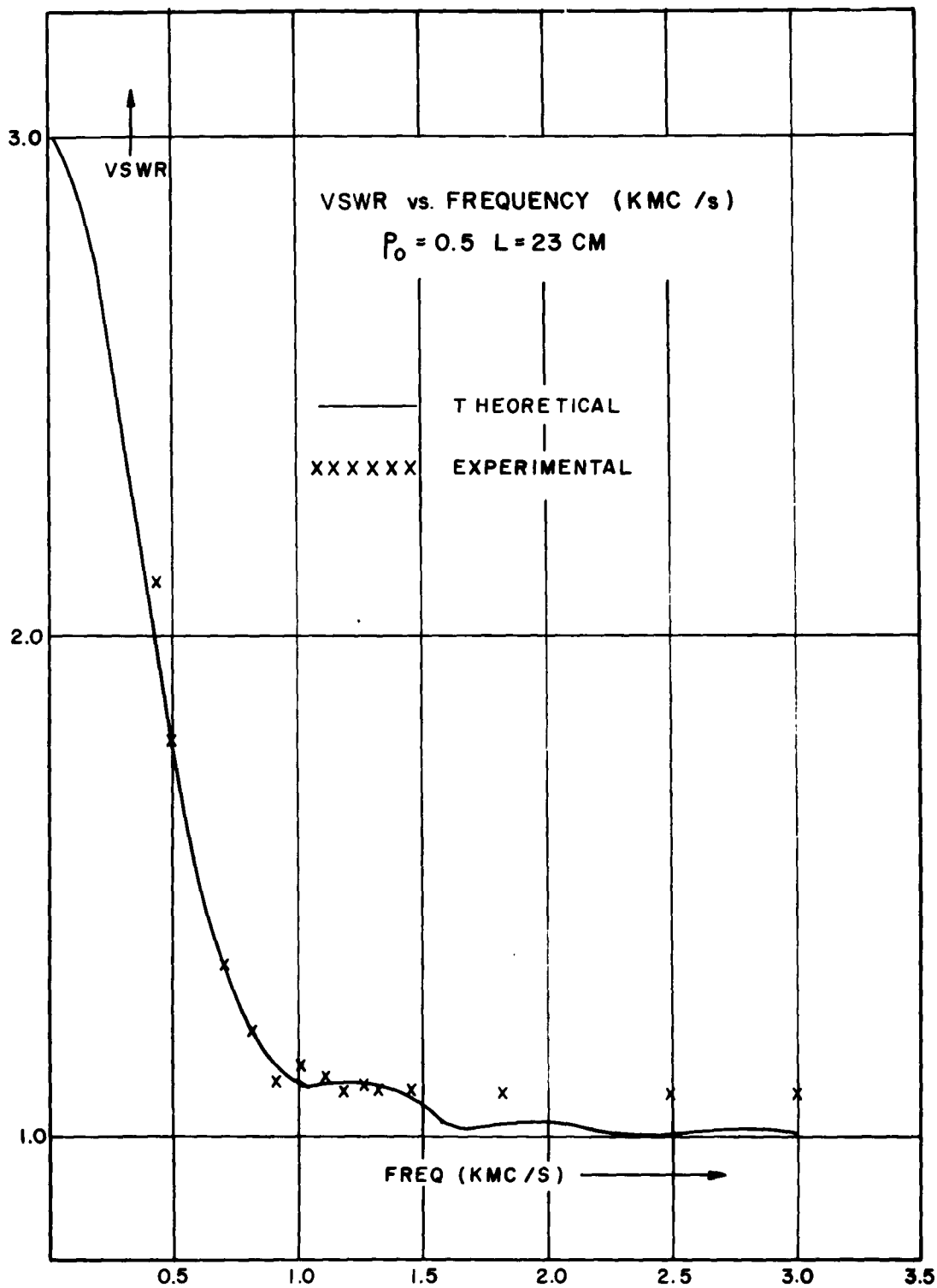

Figure 15. Comparison of Theoretical and Experimental Results for a 50 percent Mismatch.

$$(\mathrm{VSWR})^2 = 1 + \frac{1}{\sin^2\left(\frac{\pi \Delta X}{\lambda_0}\right)} \doteq \left(\frac{\lambda_0}{\pi \Delta X}\right)^2,$$

where ΔX is the distance between the half power points on either side of the minimum and λ_0 is the free space wavelength.

For the large input standing wave ratios being considered (in excess of 20), the above approximation is shown by Ginston to be less than one percent in error for computation. The experimental error in the actual measurement of ΔX for the determination of VSWR magnitude (and the determination of nodal shifts for VSWR phase) is dependent on, among other factors, the detector-amplifier sensitivity, the mechanical precision of the probe carriage, and the adjustable short, frequency instability in the r-f signal source and, not the least of all, the experimentalists' patience and fortitude. Nevertheless, the total contribution of measurement type errors is at least qualitatively available by inspection of the graphical analysis of the measured data. This valuable feature of the Deschamps method is essentially a check on the consistency and accuracy of the data used to plot the locus of the input reflection coefficient (of the combination) in the complex plane. Now, this locus is used in conjunction with the locus of the reflection coefficient of the adjustable short alone to geometrically determine the complex value of the $S_{11}(W)$ parameter of the transformer scattering matrix.

Now, in the various graphical constructions performed, inconsistent data are immediately recognized and may be discarded promptly or remeasured. Furthermore, any systematic or random errors in the data exhibit themselves in the so-called "crossover region" of the graphical data analysis. The area of this region (in general a polygon) in relation to the area of the entire complex plane used is a measure of the total accumulative experimental error. For the graphical plots and geometrical constructions that led to the experimental results of Figure 15, the ratio of areas of "crossover region" and complex plane was approximately one part in 3500. Theoretically (or ideally), this ratio is zero since the "crossover region" degenerates into a point. Finally, although no over-all quantitative experimental accuracy can be calculated, the reproducibility of the measured results by the Deschamps technique was well within three percent. Consequently, for the above reasons, the experimental accuracy is considered excellent.

At the higher frequency ranges where the predicted VSWR's are almost unity, the insertion VSWR's of the test instrumentation itself become the more prominent factors. That is to say, the VSWR of the transformer in comparison with the VSWR of the available good commercial connectors is probably smaller and thus unmeasurable with the instrumentation and techniques employed. At any rate, the data shown for the higher frequencies represent the composite VSWR due to significant contributions from the slotted line, connectors, transformer, and a slightly misfitting sliding short circuit. Thus, the theoretical performance appears to be strongly validated by the experimental results. If the experiment agrees with the theory for such a large mismatch $\rho_0 = 0.5$, then, in view of the linearizing

restriction of the theory, $|\rho(x)|^2 << 1$, the correlation between theory and experiment for smaller mismatches is assured. On this basis, then, the claims made previously would also seem to be on firm ground.

VI. CONCLUSION

A nonuniform section of coaxial transmission line has been presented. In particular, the distribution studied is expressible as a characteristic impedance with a half-period cosinusoidal function in the variable x, the direction of the TEM mode propagation. From basic considerations of the line voltage and current differential equations, an expression for the input reflection coefficient for such a nonuniform line was developed. This integral statement was evaluated for various (useful) ranges in design parameters using the Burrough's Datatron 205 computer. The resultant predicted performance of the cosinusoidal transformer indicated, in comparison to "conventional" tapers, improved over-all performance and, in some cases, outright superior performance.

The theoretical performance of the transformer was compared experimentally in a mismatch condition ($\rho_0 = 0.5$) that stretched theoretical assumptions to their limit. In this, the most severe test, the correlation between theory and experiment is excellent. For less drastic mismatch conditions, the correlation can only be better. Thus, a microwave network transformation technique is theoretically and experimentally shown to exhibit improvements in maximum bandwidth and minimum physical length over conventional coaxial tapers.

REFERENCES

1. Slater, J.C., "Microwave Transmission," McGraw Hill.
2. King, R.W.P., "Transmission Line Theory," McGraw Hill.
3. Ramo, S., Whinnery, J.R., "Field and Waves in Modern Radio," John Wiley & Sons.
4. Burrows, C.R., "The Exponential Transmission Line," BSTJ, Vol. 17, Oct 38.
5. Wheeler, H.A., "Transmission Lines with Exponential Taper," PIRE, Vol. 27, Jan 39.
6. Starr, A.T., "The Nonuniform Transmission Line," PIRE, Vol. 20, Jun 32.
7. Arnold, J.W., and Bechberger, P.F., "Sinusoidal Currents in Linearly Tapered Transmission Lines," PIRE, Vol. 19, Feb 31.
8. Yang, "Parabolic Transmission Line," PIRE, Aug 55.
9. Pierce, J.R., "A Note on the Transmission Line Equations in Terms of Impedance," BSTJ, Vol. 22, Jul 43.
10. Walker, J.R., and Wax, N., "Nonuniform Transmission Lines and Reflection Coefficients," J. App. Phys., Vol. 17, Dec 46.
11. Bolinder, F., "Fourier Transforms and Tapered Transmission Lines," PIRE, Vol. 44, Apr 56.
12. Latmiral, G., and Vinciquerra, R., "Nonuniform Transmission Lines and Broadband Microwave Absorbers," RADC-TN-61-142 and RADC-TN-59-195, Contract No. AF61(052)-36.
13. Bolinder, F., "Fourier Transforms in the Theory of Inhomogeneous Transmission Lines," *Transactions of the Royal Institute of Technology*, Stockholm, Sweden, No. 48, 1951.
14. Klopfenstein, R.W., "A Transmission Line Taper of Improved Design," PIRE, Vol. 44, Jan 56.
15. Scott, H.J., "The Hyperbolic Transmission Line as a Matching Section," PIRE, Vol. 44, pp. 1654-1657, Nov. 53.
16. King, R.W.P., "Transmission Line Theory," McGraw Hill, p. 359, eqs. (4) and (9).
17. Deschamps, G.A., "Application of Non-euclidean Geometry to the Analysis of Wave Guide Junctions." Report URSI-IRE, Spring Meeting, 1952.
18. Storer, J.E., Sheingold, L.S., and Stein, S., "A Simple Graphical Analysis of Wave Guide Junctions," PIRE, 41, 1004, 1953.
19. Ginston, E.L., "Microwave Measurements," McGraw Hill, pp 266-268.

BIBLIOGRAPHY

Bronwell, A.B., and Beam, R.E., "Theory and Application of Microwaves," McGraw Hill.

Guillamin, E.A., "Communication Networks," Vol I, John Wiley and Sons.

King, R.W.P., "Transmission Line Theory," McGraw Hill.

Ragan, G.L., "Microwave Transmission Circuits," MIT Radiation Laboratory Series, McGraw Hill.

Ramo, S., and Whinnery, J.R., "Fields and Waves in Modern Radio," John Wiley and Sons.

Sarbacher, R.I., and Edson, W.A., "Hyper-and-Ultrahigh Frequency Engineering," John Wiley and Sons.

Skilling, H.H., "Fundamental of Electric Waves," 2nd Edition, John Wiley and Sons.

Slater, J.C., "Microwave Transmission," McGraw Hill.

APPENDIX

The equation to be solved is:

$$\frac{d\rho}{dx} - 2\gamma\rho + \frac{1}{2}\frac{d}{dx}\ln Z_0(x) = 0; \tag{A-1}$$

let

$$\rho(x) = A \exp\left[2\int_{x_0}^{x}\gamma(\xi)\,d\xi\right] + u(x)\exp\left[2\int_{x_0}^{x}\gamma(\xi)\,d\xi\right], \tag{A-2}$$

where A is a constant and x_0 a reference point on the closed interval $[0, L]$. Differentiating (A-2).

$$\frac{d\rho}{dx} = 2A\gamma(x)\exp\left[2\int_{x_0}^{x}\gamma(\xi)\,d\xi\right] + 2u\gamma\exp\left[2\int_{x_0}^{x}\gamma(\xi)\,d\xi\right] + \frac{du}{dx}e^{2\int_{x_0}^{x}\gamma(\xi)\,d\xi} \tag{A-3}$$

Upon substitution of (A-2) and (A-3) in equation (A-1) and after simplification, we have the differential equation for $u(x)$:

$$\frac{du}{dx}\exp\left[2\int_{x_0}^{x}\gamma(\xi)\,d\xi\right] + \frac{1}{2}\frac{d}{dx}(\ln Z_0) = 0. \tag{A-4}$$

Introducing the dummy variable t for x in the above and solving, one arrives at:

$$u(x) = -\frac{1}{2}\int_{x_0}^{x}\frac{d}{dt}[\ln Z_0(t)]\exp\left[-2\int_{t_0}^{t}\gamma(\xi)d\xi\right]dt. \tag{A-5}$$

Thus, the solution to (A-1) aside from the constant A, is:

$$\rho(x) = \exp\left[2\int_{x_0}^{x}\gamma(\xi)\,d\xi\right]\left\{A - \frac{1}{2}\int_{x_0}^{x}\frac{d}{dt}[\ln Z_0(t)]\exp\left[-2\int_{t_0}^{t}\gamma(\xi)d\xi\right]dt\right\}. \tag{A-6}$$

To evaluate the constant A, set $x = L$. Thus,

$$\rho(L) = \exp\left[2\int_{x_0}^{L}\gamma(\xi)\,d\xi\right]\left\{A - \frac{1}{2}\int_{x_0}^{L}\frac{d}{dt}[\ln Z_0(t)]\exp\left[-2\int_{t_0}^{t}\gamma(\xi)d\xi\right]dt\right\}, \tag{A-7}$$

or

$$A = \rho(L)\exp\left[-2\int_{x_0}^{L}\gamma(\xi)\,d\xi\right] + \frac{1}{2}\int_{x_0}^{L}\frac{d}{dt}[\ln Z_0(t)]\exp\left[-2\int_{t_0}^{t}\gamma(\xi)\,d\xi\right]dt. \tag{A-8}$$

Substituting this expression into (A-6), we arrive at the general solution:

$$\rho(x) = \rho(L)\exp\left[-2\int_{x}^{L}\gamma(\xi)\,d\xi\right] +$$

$$\frac{1}{2}\exp\left[2\int_{x_0}^{x}\gamma(\xi)\,d\xi\right]\left\{\int_{x_0}^{L}\frac{d}{dt}[\ln Z_0(t)]\exp\left[-2\int_{t_0}^{t}\gamma(\xi)\,d\xi\right]dt\right\}. \tag{A-9}$$

CATALOGUE FILE CARD

Rome Air Development Center, Griffiss AF Base, N.Y.
Rpt No. RADC-TDR-63-17. A NONUNIFORMLY DISTRIBUTED PARAMETER MATCHING NETWORK FOR THE MICROWAVE FREQUENCIES. 32p. incl illus.

Unclassified Report

A nonuniform section of coaxial transmission line is investigated as an impedance matching network. Assuming that the purity of the dominant transverse electromagnetic (TEM) mode is maintained, the coaxial transformer section proposed is one in which the distributed series inductance and shunt capacitance are prescribed mathematical functions of the axial cylindrical coordinate, that is, the direction of propagation. These variations are expressed as a variable characteristic impedance in the explicit form of a half-period cosinusoidal distribution.

1. Microwaves
2. Electromagnetic Waves
I. Project No. 8505
II. D.J. Kenneally
III. In ASTIA collection

Rome Air Development Center, Griffiss AF Base, N.Y.
Rpt No. RADC-TDR-63-17. A NONUNIFORMLY DISTRIBUTED PARAMETER MATCHING NETWORK FOR THE MICROWAVE FREQUENCIES. 32p. incl illus.

Unclassified Report

A nonuniform section of coaxial transmission line is investigated as an impedance matching network. Assuming that the purity of the dominant transverse electromagnetic (TEM) mode is maintained, the coaxial transformer section proposed is one in which the distributed series inductance and shunt capacitance are prescribed mathematical functions of the axial cylindrical coordinate, that is, the direction of propagation. These variations are expressed as a variable characteristic impedance in the explicit form of a half-period cosinusoidal distribution.

1. Microwaves
2. Electromagnetic Waves
I. Project No. 8505
II. D.J. Kenneally
III. In ASTIA collection

Rome Air Development Center, Griffiss AF Base, N.Y.
Rpt No. RADC-TDR-63-17. A NONUNIFORMLY DISTRIBUTED PARAMETER MATCHING NETWORK FOR THE MICROWAVE FREQUENCIES. 32p. incl illus.

Unclassified Report

A nonuniform section of coaxial transmission line is investigated as an impedance matching network. Assuming that the purity of the dominant transverse electromagnetic (TEM) mode is maintained, the coaxial transformer section proposed is one in which the distributed series inductance and shunt capacitance are prescribed mathematical functions of the axial cylindrical coordinate, that is, the direction of propagation. These variations are expressed as a variable characteristic impedance in the explicit form of a half-period cosinusoidal distribution.

1. Microwaves
2. Electromagnetic Waves
I. Project No. 8505
II. D.J. Kenneally
III. In ASTIA collection

Rome Air Development Center, Griffiss AF Base, N.Y.
Rpt No. RADC-TDR-63-17. A NONUNIFORMLY DISTRIBUTED PARAMETER MATCHING NETWORK FOR THE MICROWAVE FREQUENCIES. 32p. incl illus

Unclassified Report

A nonuniform section of coaxial transmission line is investigated as an impedance matching network. Assuming that the purity of the dominant transverse electromagnetic (TEM) mode is maintained, the coaxial transformer section proposed is one in which the distributed series inductance and shunt capacitance are prescribed mathematical functions of the axial cylindrical coordinate, that is, the direction of propagation. These variations are expressed as a variable characteristic impedance in the explicit form of a half-period cosinusoidal distribution.

1. Microwaves
2. Electromagnetic Waves
I. Project No. 8505
II. D.J. Kenneally
III. In ASTIA collection